Dysfunctional endothelial cells directly stimulate cancer inflammation and metastasis

Citation: Franses, Joseph W., Natalia C. Drosu, William J. Gibson, Vipul C. Chitalia, and Elazer R. Edelman. "Dysfunctional Endothelial Cells Directly Stimulate Cancer Inflammation and Metastasis." Int. J. Cancer 133, no. 6 (April 8, 2013): 1334–1344.

As Published: http://dx.doi.org/10.1002/ijc.28146

Publisher: John Wiley & Sons, Inc/Union for International Cancer Control

Persistent URL: http://hdl.handle.net/1721.1/92360

Version: Author's final manuscript: final author's manuscript post peer review, without publisher's formatting or copy editing

Published in final edited form as:
Int J Cancer. 2013 September 15; 133(6): 1334–1344. doi:10.1002/ijc.28146.

Dysfunctional endothelial cells directly stimulate cancer inflammation and metastasis

Joseph W. Franses[1], **Natalia C. Drosu**[1], **William J. Gibson**[1], **Vipul C. Chitalia**[2], and **Elazer R. Edelman**[1,3,*]

[1]Harvard–MIT Division of Health Sciences and Technology, MIT, E25-438, Cambridge, Massachusetts 02139

[2]Renal Section, Department of Medicine, Boston University School of Medicine, Boston, Massachusetts 02118

[3]Cardiovascular Division, Department of Medicine, Brigham and Women's Hospital, Harvard Medical School, Boston, Massachusetts 02115

Abstract

Although the influence of context-dependent endothelial cell regulation of vascular disease and repair is well-established, the privileged roles endothelial cells play as paracrine regulators of tumor progression has only recently become appreciated. We hypothesized that if the same endothelial physiology governs vascular and cancer biology then endothelial cell control in cancer should follow endothelial regulation of vascular health. Healthy endothelial cells promote vascular repair and inhibit tumor invasiveness and metastasis; dysfunctional endothelial cells have the opposite effects. We now ask if dysfunctionally activated endothelial cells will promote cancer cell inflammatory signaling and aggressive properties. Indeed, while factors released from quiescent ECs induce balanced inflammatory signaling, correlating with decreased proliferation and invasiveness, factors released from dysfunctional ECs robustly activated NF-κB and STAT3 signaling within cancer cells, correlating with increased *in vitro* invasiveness and decreased proliferation and survival. Furthermore, matrix-embedded dysfunctional endothelial cells stimulated intratumoral pro-inflammatory signaling and spontaneous metastasis, while simultaneously slowing net primary tumor growth, when implanted adjacent to Lewis lung carcinoma tumors. These studies may broaden our realization of the roles of endothelial function and dysfunction, increase understanding and control of the tumor microenvironment, and facilitate optimization of anti-angiogenic and vascular-modifying therapies in cancer and related diseases.

Keywords

angiogenesis; endothelium; inflammation; metastasis

Introduction

Endothelial cells (ECs) control vascular repair, and vascular health is defined by endothelial integrity.[1] Healthy or "quiescent" ECs promote vascular repair, limiting EC injury restricts vascular disease, and vascular healing is enhanced when EC injury is contained[2] or when

Corresponding author: Professor Elazer R. Edelman, 77 Massachusetts Avenue, E25-438, Cambridge, MA 02139.; tel 617-253-1569; fax 617-253-2514; ere@mit.edu.

Conflicts of interest: E.R.E. and J.W.F. are co-inventors on a patent application owned by Massachusetts Institute of Technology that describes the use of cell implants to modulate cancer behavior. E.R.E. is a founder of Pervasis Therapeutics, which has licensed the patent application. No other authors have competing interests to declare.

injured endogenous ECs are replaced by exogenous EC implants.[3] The contranegative is true as well – diseased or "dysfunctional" ECs exacerbate vascular injury. Such EC paracrine regulatory control should not be restricted to the macrovasculature as ECs are part of every tissue, lining not only the luminal surface of large vessels but also the perfusing microvasculature of every organ. Indeed, ECs also regulate the repair of organs much as they do arteries.[4]

The acknowledged roles of ECs in tumor biology continue to evolve. Endothelial disarray, as part of vascular structural abnormalities, contributes to abnormal intra-tumoral perfusion and a vicious cycle of local hypoxia, impaired permeability, extracellular matrix degradation and efflux of cancer cells.[5] That healthy ECs also limit cancer cell proliferation and invasion through biochemical regulation analogous to vascular healing adds an element to this continuum.[6] Questions arise whether regulation is restricted to the control imposed by healthy ECs and whether paracrine interactions induce dysfunctional ECs to promote, not simply permit, disease progression. We hypothesize that "dysfunctional" (i.e. inflamed and otherwise pathologically activated) ECs stimulate cancer aggressiveness like they promote vascular disease, not only from loss of regulatory ECs but from the stimulation of pathologic processes by dysfunctional ECs.[7] Moreover, we propose that the pro-inflammatory and hyper-activated intratumoral milieu modulates EC paracrine secretion, transforming the EC phenotype from quiescent and disease-inhibitory to dysfunctionally activated and disease-stimulatory.

We examined the response of cancer cells in culture and in murine tumors to pathologically deranged "dysfunctional" ECs (DECs) using a model system inspired by both vascular and tumor biology paradigms. Although important factors like biomechanical stress[8], hypoxia[9], and presence of other stroma[10] are not directly modeled herein, DECs share many phenotypic features with dysfunctional ECs from the atherosclerosis milieu[11, 12] and ECs harvested directly from tumors.[13] Our studies should help to expand the "angiocrine" tumor-regulatory paradigms, expand analogies between EC paracrine regulatory mechanisms in the fields of non-malignant vascular disease and tumor biology, and aid in the design of more effective therapies that target or utilize endothelial cells in a range of disease states.

Materials and Methods

Reagents

Antibodies to NF-κB p65 and p-p65, integrin β3, VE-cadherin, p-TIE2, p-STAT3, cleaved PARP, fibrillarin, GAPDH, β-actin, and α-tubulin were from Cell Signaling Technology. The CD11b antibody was from Abcam. Antibodies to perlecan, VE-cadherin, VEGFR2, and NF-κB p65 (immunofluorescence) and HRP-conjugated secondary antibodies were from Santa Cruz Biotechnology. The antibody to eNOS was from Abcam. Fluorescently-labeled secondary antibodies and calcein-AM were from Invitrogen. Recombinant human TNF-α was from BioLegend; VEGF and FGF2 were from Invitrogen. BAY 11-7082 was from Cayman Chemicals.

Cell culture

A549, NCI-H520, HOP62, and HOP92 lung carcinoma cells and THP-1 (monocytic leukemia) cells (ATCC) were cultured in RPMI with 10% FBS, 100 U/mL penicillin, and 100 μg/mL streptomycin. Human umbilical vein ECs (HUVECs, Invitrogen) were cultured in EGM-2 (Lonza) with 5% FBS on gelatin-coated plates, passages 3–6. EC-conditioned media were generated from confluent HUVEC monolayers by 48 hours of culture in MCDB131 (Invitrogen) with 10% FBS, 100 U/mL penicillin, and 100 μg/mL streptomycin; cell morphologic phenotype was stable during the conditioning period. Cells and debris were

removed by centrifugation (5 minutes, 500g) and media aliquotted and stored at −80°C. Conditioned medium (48 hr, 6 mL EGM-2 per 10-cm dish) pooled from the four cancer cell lines grown to confluence replaced 33% of the volume of EGM-2. 10 ng/mL TNF-α, 10 ng/mL VEGF, and 1 ng/mL FGF-2 was added to comprise the "dysfunctional" EC (DEC) growth medium - a modification of a published protocol used to generate surrogate "tumor-associated" ECs in culture.[13]

Matrix-embedded ECs (MEECs) were generated by culturing ECs within sterile Gelfoam compressed matrices (Pfizer, New York).[4] ECs were seeded onto hydrated 1.25×1×0.3 cm blocks and allowed to attach for 1.5 hours before seeding the contralateral side. Two blocks were added to 30-mL polypropylene tubes and cultured for up to 3 weeks. Samples from each lot were digested with collagenase (type I, Worthington Biochemicals) and seeding efficiency determined with a Z1 particle counter (Beckman Coulter). Cell viability was assessed by trypan blue exclusion.

In vitro cell number, proliferation, apoptosis, tube-forming, permeability, monocyte adhesion, and invasion/migration assays

Cell number—Cells were detached with trypsin and counted with a Z1 Coulter particle counter (Beckman Coulter). Alternatively, the reduction of MTS reagent (Promega) was monitored per the manufacturer's instructions.

Proliferation—Incorporation of BrdU was monitored via BrdU ELISA (Cell Signaling Technology) per the manufacturer's instructions.

Apoptosis—Caspase-3/7 activity was examined using the ApoONE kit (Promega) per the manufacturer's instructions.

Tube forming—15,000 ECs were seeded in each well of 96-well plate coated with 50 μL of Matrigel (BD Biosciences). After 16–20 hours, tube/cord formation was imaged by phase contrast microscopy and tube length in the central low-power field quantified by ImageJ.

Monolayer permeability—ECs were seeded onto transwell inserts (0.4 μm pores, BD Biosciences) and grown to post-confluence in 4 days. Then the medium in the upper chamber was changed to EGM-2 plus 0.1 mg/mL FITC-dextran (70 kD, Sigma), and medium in the lower chamber was changed to fresh EGM-2. Diffusion was allowed to occur for 1 hour at 37°C, after which the inserts were removed and an aliquot was taken from the lower chamber for quantification with a Varioskan Flash instrument (Thermo), with concentration calculated from a standard curve. Results were normalized per EC in the control condition.

Monocyte adhesion—ECs were seeded onto gelatin-coated 24-well plates and grown to post-confluence over 4 days. 5×10^5 calcein AM-labeled THP-1 cells in 100 μL of RPMI were seeded onto the monolayers and allowed to adhere for one hour at 37°C. Nonadherent cells were removed by gentle washing with PBS, and monolayers were lysed in 0.1% SDS and lysates were transferred to an optically neutral 96-well plate. Fluorescent signal was measured with a Varioskan Flash plate reader (Thermo), with background from EC monolayers without THP-1 cells subtracted from all measurements and results normalized per EC in the control condition.

Invasion/migration—Chemoinvasion kits (BioCoat, BD) were used per the manufacturer's instructions. Invaded or migrated cells adherent to the bottom of the inserts were fixed, stained with DAPI (1 μg/mL, 30 minutes) and imaged by epifluorescence

microscopy. Images were analyzed by visual inspection and cytometric quantification of 4 random 20X fields at the microscope or by using the "particle counter" feature of ImageJ for the central 10X field. Data are expressed as an invasion index[14], the average number of invaded cells and the average number of migrated cells of a given condition, normalized to the control condition with at least 3 wells used per condition.

Gene expression analysis

Total RNA was purified (RNEasy Mini Plus, Qiagen) and cDNA synthesized (TaqMan reverse transcription reagents, Applied Biosystems) using 1 μg of RNA per sample. Real-time PCR analysis was performed (Opticon II instrument, MJ Research) using SYBR Green PCR Master Mix (Applied Biosystems) and appropriate primers (Table 1). Gene expression was quantified using the ΔΔCt method, with 18SRNA or GAPDH as a housekeeping gene. qPCR primer arrays (Lonza) were used for medium-throughput gene expression analysis.

Protein expression analysis

Whole cell extracts were harvested in 0.5% Triton X-100, 0.1% SDS, protease inhibitor cocktail (Roche), 2 mM sodium orthovanadate, 50 mM sodium fluoride, and 4 mM PMSF. Nuclear and cytoplasmic protein fractions were obtained as described elsewhere.[15] Samples were separated on glycine-SDS gels, transferred to nitrocellulose membranes, immunoblotted with the appropriate primary and HRP-conjugated secondary antibodies, and detected with a chemiluminescent peroxidase substrate (Luminata Forte, Millipore) for luminescence detection with a FluorChem luminometer (Alpha Innotech; CA) and analysis with ImageJ. A cytokine antibody array (RayBiotech; GA) was used per the manufacturer's instructions for assessment of cell biosecretions. Array luminescence was imaged using a FluorChem luminometer and quantified with ImageJ. Quantification of individual secreted factors present in cell supernatants was via ELISA (RnD Systems; MN) per the manufacturer's specifications.

For immunofluorescence imaging, cells were fixed in paraformaldehyde and stained with primary antibodies and AlexaFluor 594-conjugated secondary antibodies (Invitrogen); nuclei were counterstained with DAPI. Images were acquired with a Nikon microscope and analyzed using either ImageJ (NIH) or CellProfiler (Broad Institute).

Murine tumor model

All animal experiments were approved by the MIT Committee on Animal Care in compliance with NIH guidelines. Female C57BL6 mice, ~6 weeks of age (Jackson Laboratories) were used in the Lewis lung carcinoma (LLC) implantation-resection-metastasis model, in which early metastases are suppressed by angiostatin elaborated from the primary tumor; hence removal of the primary tumor allows macroscopic growth of lung metastases.[16] Lewis lung carcinoma cells (ATCC) were passaged serially through mice for two generations before use to bolster metastatic capacity, then 10^6 LLC cells were injected in the subcutaneous dorsum. After 6 days for tumor engraftment, acellular matrix (control), MEECs (~1E6 cells per animal), or dysfunctional MEECS (D-MEECs, ~1E6 cells per animal) were implanted adjacent to tumors, which were ~30 mm^3 in volume. After 8 additional days, tumors and implants were excised. 14 days after the resection, the animals were sacrificed by CO_2 inhalation. 2% isoflurane anesthesia was administered via nose cone and 0.1 mg/kg buprenorphine administered perioperatively. Tumor dimensions were measured with Vernier calipers, using two orthogonal measurements to estimate volume assuming prolate spheroid geometry.

Statistical analysis

Experiments were performed at least thrice for validation and each time in triplicate, at minimum. Results are expressed as mean ± SEM. Comparison of two groups was performed using a student's t-test. Comparison of >2 groups was performed using ANOVA followed by t-tests. $p<0.05$ was taken as statistically significant.

Results

Dysfunctionally activated endothelial cells (DECs) have dysregulated phenotypes

Our "DECs" were stimulated with a combination of factors mimicking various aspects of the tumor microenvironment (cancer-secreted factors, angiogenic factors, and a pro-inflammatory cytokine). The DECs were generated using a modification of a protocol used to create surrogate tumor ECs, which have similar gene expression profiles to ECs harvested directly from tumors.[13] DECs grew more slowly in culture, with 42±2% fewer cells at confluence than control "quiescent" (meaning healthy, not referring to proliferative rate in culture) ECs (p=0.002, Fig. 1A), and were larger with a mesenchymal morphology, unlike the cobblestone appearance of quiescent postconfluent ECs (Fig. 2B). Relative to ECs, DECs formed tubes less efficiently on Matrigel (26±9% reduction, p=0.007, Fig. 1B), had dramatically increased permeability (2.5±0.4-fold p=0.036, Fig. 1C), and higher avidity for binding THP-1 monocytes (4.4±0.3-fold, $p=3.5*10^{-7}$, Fig 1D). Indices of endothelial activation were increased and of quiescence reduced (Fig 2A). DECs possessed, relative to control ECs, increased phosphorylation of VEGFR2 (8.7±2.6 fold increase, p=0.022) and total integrin β3 (2.3±0.4 fold increase, p=0.023), and decreased VE-cadherin (39±12% decrease, p=0.04), and phosphorylated Tie2 (81±7% decrease, p=0.009). eNOS protein expression was also downregulated in DECs (92±1% decrease, $p=8.5*10^{-6}$), although possible compensatory increases in eNOS activity were not examined in this work. Further, localization of signaling proteins changed, with a 67±12% decrease in surface-localized and cytoplasmic VEGFR2 and an 84±6% decrease in VE-cadherin in DECs relative to ECs ($p < 0.05$ for each, Fig. S2).

DECs showed a 10-fold increase in the percentage of cells with NF-κB p65 nuclear localization after 4 days of culture (p=0.005, Fig. 2B), suggesting a sustained pro-inflammatory state. These results were verified by examination of the nuclear and cytoplasmic protein fractions from ECs and DECs (Fig. S1): DEC nuclei contained ~3.5 times more NF-κB p65 and STAT3β than EC nuclei. Additionally, DECs showed very low expression of intact perlecan (Fig. 2B), a molecule important for maintaining the quiescent EC phenotype.[6, 17]

The gene expression profile of DECs is pro-inflammatory and pro-thrombotic

As ECs adopt a mesenchymal morphology in association with endothelial-to-mesenchymal transition (EndMT) and may play a role in inflammatory and tumor-associated states[18, 19] we examined gene expression changes of EndMT-associated transcription factors in DECs. There were ~3-fold increases in the levels of Snail and Twist transcripts (each $p<0.05$, Fig. S3) and widespread changes in the DEC transcriptome relative to that of EC controls (Fig. 2C). The expression of many pro-inflammatory NF-κB target genes – e.g. GM-CSF, IL-8, IL-6, and E-selectin – were significantly increased, the expression of quiescence-promoting, anti-inflammatory genes – e.g. eNOS, VE-cadherin, Ang1 – were decreased, the expression of leukocyte adhesion molecules VCAM1 and ICAM1 were increased, and the balance of coagulation-related genes shifted toward a pro-coagulant state (higher tissue factor, TF, and lower thrombomodulin, THBD). Analysis of protein secretion by cytokine blots (Fig. 2D) of ECs and DECs corroborated and extended the identified gene expression changes: DECs secreted much higher amounts of pro-inflammatory cytokines MCP-1, IL-6, IL-8, GRO-α/

CXCL1, RANTES, G-CSF, MCP-2, GM-CSF, and MCP-3. Importantly, although the culture cocktail used to generate "DECs" contained 10 ng/mL TNF-α, this protein was undetectable in DEC-conditioned media, indicating that exogenous TNF-α was removed by washing before conditioned media collection. It is likely that the other EC-activating factors were similarly removed before conditioning.

We analyzed the expression of selected genes in ECs treated for four days with the individual (cancer cell secretions, TNF-α, VEGF, FGF2) components of the DEC cocktail to discriminate their specific effects on EC gene expression (Fig. S4A). Replacement of 33% of the culture medium with media from cancer cells had similar effects to TNF-α (10 ng/mL) alone, and when combined with TNF-α recapitulated most of the effect of the complete cocktail. However, as evidenced for example by eNOS gene expression, the complete cocktail was more effective in altering EC gene expression profiles than individual components. EC gene expression profile was not dramatically changed by sustained culture in saturating concentrations of VEGF and FGF2, implying a resistance by postconfluent ECs to pro-angiogenic activation.

Cancer cell proliferation, apoptosis, inflammation, and invasiveness

Quiescent ECs inhibit the proliferation and invasiveness of cancer cells, much like they control vascular smooth muscle hyperplasia and monocyte recruitment, in a manner that correlates with steady-state inhibition of pro-inflammatory signaling and is reversed with targeted disruption of the healthy EC phenotype.[6] Since the DEC phenotype was highly deranged and pro-inflammatory, we hypothesized that DECs would be cancer-stimulatory along multiple axes.

The net growth of three different cancer lines was significantly inhibited by EC media, ($p<0.003$, Fig. 3A), and even further by DEC media (~80% reduction, $p<3*10^{-7}$ for all versus control; $p<0.04$ for all versus EC media). Inhibition of cancer growth correlated with a ~20% reduction in BrdU incorporation for both EC- and DEC-conditioned media ($p<0.05$ versus control for all cancer cell lines, Fig. 3B). DECs, unlike ECs, robustly induced apoptosis as detected by an assay for caspase-3/7 activity (3.4±0.4-fold versus control for A549, 1.7±0.1-fold for NCI-H520, and 2.4±0.2-fold for HOP62 relative to control). These results were verified further in A549 cells by Western blot analysis of cleaved and total PARP ($p=0.013$ versus control, $p=0.033$ versus EC, Fig. 3C). Although the DEC secretome contains ~5-fold more IL-6, than the EC secretome (Fig. 2D), and IL-6 can itself induce cancer cell apoptosis[20], the enhanced stimulation of cancer cell apoptosis by DEC medium was not inhibited by neutralization of IL-6 activity (Fig S5).

Pro-inflammatory signaling in cancer cells has been implicated in many facets of the disease[15, 21], and though cytokines such as IL-6 can kill cancer cells, those that survive tend to be particularly aggressive and metastatic.[20] Therefore we examined signaling through the STAT3 and NF-κB pathways in A549 lung carcinoma cells after variable time in EC or DEC-conditioned media culture (Fig. 4A). DECs increased STAT3 phosphorylation at 24 hours 6.2±0.8-fold ($p=0.0006$), which inverted to a 79±3% decrease ($p=0.0002$) by 96 hours. Secretions from quiescent ECs in contrast only minimally activated STAT3 in A549 cells at 24 hours (1.7±0.3-fold, $p=0.049$) that inverted to a 46±14% ($p=0.037$) decrease by 96 hours. Similarly, there was a 1.7±0.1-fold increase ($p=0.035$) in NF-κB p-P65 induced by DEC-conditioned media at 4 hours that increased to 5.0±0.8 fold by 24 hours ($p=0.0046$) and remained elevated at 96 hours ($p=0.01$). Here too EC media induced a smaller pro-inflammatory response, with a trend toward ($p=0.075$) increased p-P65 at 24-hrs and moderate sustained activation at 96 hours ($p=0.0055$). Intriguingly, the observed changes in NF-κB activation caused by EC media were associated with a 1.6±0.4-fold increase ($p=0.047$) in IκBα at 24 hours, supporting the notion of a controlled, balanced activation of

cancer cell inflammatory pathways by EC secretions. We examined a subset of the p-STAT3 and p-P65 Western blots for A549 cells NCI-H520 and HOP62 cells (Fig. S7), and the additional results agreed with our findings in A549 cells (Fig. S7). In all experiments we normalized phosphoprotein Western blot data with either tubulin or actin, rather than to the total quantities of the signaling proteins, since the concentrations of these species were constant over a time period of days.

Intense stimulation of pro-inflammatory signaling in A549 cells by DEC media might stimulate invasive properties, an *in vitro* correlate of metastasis. As in prior studies[6] media from quiescent ECs inhibited *in vitro* invasiveness of A549 cells by 33±10% ($p<0.005$, Fig. 4B), but DECs stimulated A549 invasiveness by 39±18% ($p<0.01$, Fig. 4B). These effects correlated directly ($r^2 = 0.93$, Fig. 4D) with a 32±7% decrease in A549 nuclear NF-κB immunofluorescent staining by culture in EC media ($p=0.037$, Fig. 4C) and a 2.1±0.4-fold increase by DEC media ($p=0.022$, Fig. 4C). Indeed, inhibition of NF-κB nuclear translocation with an irreversible inhibitor of IkBa phosphorylation[22] reversed the ability of DEC media to stimulate A549 invasiveness (Fig. S6).

Together, our results suggest a controlled, sustained anti-proliferative and anti-invasive effect on cancer cells by quiescent ECs and a pro-inflammatory, invasion-stimulatory effect on cancer cells by dysfunctional ECs.

Adjacent D-MEECs stimulate spontaneous metastasis

We used the Lewis lung carcinoma implantation-resection-metastasis model to examine EC-cancer *in vivo* regulation (Fig. S8). Although a heterotopic xenograft, the model allows for facile surgical access and robust spontaneous metastasis.[16] We generated matrix-embedded quiescent ECs (MEECs) or dysfunctional ECs (D-MEECs) by prolonged culture in the same cocktail used to create *in vitro* DECs. We have previously showed that use of such implantable endothelial constructs allows sustained implant viability and does not engender a host immunological rejection.[23] The D-MEEC phenotype was altered relative to MEEC phenotype in a manner similar to DECs versus ECs (Fig. S9).

D-MEEC implants had significant effects on the behavior of adjacent tumors. Tumor volumes were equal (~30 mm^3) at MEEC/D-MEEC implantation. Adjacent D-MEEC implants reduced tumor volumes 14 days post-implant by 54±14% relative to controls ($p=0.048$, Fig. 5A). Reduction in size correlated with a 68±10% reduction in Ki67 labeling index ($p=0.02$, Fig. 5B) and a 67±13% increase in the number of cleaved caspase-3 events per 10X field ($p=0.0001$, Fig. 5C). In concert with defined effects of quiescent EC implants, MEECs induced a 39±9% lower Ki67 index than control implants ($p=0.006$, Fig. 5B) but no gross effects on Lewis lung tumor growth or metastasis.

Inflammatory markers were also affected by adjacent endothelial implants. Concomitant with reduction in primary tumor size by D-MEECs, there was a 16±5% increase ($p=0.011$, Fig. 5D) in the fraction of nuclei within tumor cryosections that stained for NF-κB p65. This increase in inflammatory signaling correlated with increase in the metastatic properties of the D-MEEC treated Lewis lung primary tumors. Four of five animals in this group had macroscopic lung metastatic nodules involving all lung lobes, and the same animals each had regional cervical metastatic tumors ($p<0.05$ each by proportion z-test). Only one of five animals in the acellular control matrix group exhibited regional recurrence and macroscopically identifiable lung nodules. Although there was a 23±4% reduction ($p=0.0002$, Fig. 5D) in inflammatory signaling within MEEC-treated primary tumors, there was no reduction in metastasis relative to the control group in these animals. Differences in tumor behavior induced by adjacent MEEC or D-MEEC implants could not be explained by macrophage recruitment (Fig. S10). Thus, adjacent D-MEEC implants directly affected the

egress of blood-borne, metastatic cancer cells most likely via elaboration of pro-inflammatory factors such as those identified in vitro.

These results support our *in vitro* results and demonstrate that biochemically "dysfunctional" EC implants can retard tumor growth but enable metastasis, presumably from stimulation of pro-inflammatory signaling pathways in the cancer cells.

Discussion

ECs line every vessel, sensing and biochemically responding to flow from above, strain and stress from below and local density at their periphery. These vantage points allow regulation of multiple aspects of local biology. The dynamic response of the EC secretome to microenvironmental perturbations allows the EC to provide a range of paracrine effects. This capability, entrenched in our understanding of vascular disease, has re-emerged in tumor biology.[24] We recently demonstrated paracrine regulatory effects of ECs in cancer. Quiescent ECs – similar to those that inhibit vascular smooth muscle hyperplasia and thrombosis after vascular injury[25, 26] – inhibited *in vitro* cancer proliferation and invasiveness, and *in vivo* tumor growth and metastasis[6].

We now show that dysfunctionally activated ECs can robustly promote the pro-inflammatory signaling within and hence the invasiveness of cancer cells. The isolated phenotype of our *in vitro* "dysfunctional" ECs is similar to the dysfunctional ECs of macrovascular disease[7] and tumor-derived ECs.[13] Activated integrin (e.g. integrin β3) and extracellular matrix expression[27], dysregulated leukocyte adhesion (e.g. by altering expression of E-selectin, VCAM-1, etc.)[28], abnormal responses to oxidative stress[29], and abnormal response to the mechanical microenvironment[30] likely arise from pathologically activating stimuli common to both the tumor[21, 31, 32] and atherosclerotic milieux.[33, 34] Thus, the paracrine effects of dysfunctional ECs are useful in examining cell-cell crosstalk in cancer, atherosclerosis, and other diseases, with the caveat that no *in vitro* model can fully recapitulate the complex anatomy and physiology of any tissue.

Continued examination of paracrine effects of dysfunctional ECs adds to work investigating the contribution of inflammatory signaling to tumor progression.[31, 32] The NF-κB[15] and STAT3[21] signaling pathways are particularly important in controlling cancer-stimulatory pro-inflammatory signals relevant for tumor growth and metastasis. Activation of these pathways profoundly affects cancer cells and tumor stroma.[35] We observed activation of the inflammatory pathways in a stromal cell (the EC) inducing NF-κB activation in cancer cells, leading to increased cancer invasion and metastasis. Recently, Pitroda et al demonstrated that tumor endothelial inflammatory signatures correlate with prognosis.[36]

Further, the dynamics of inflammatory signaling may be particularly important in cancer-stroma crosstalk interactions. NF-κB-induced transcriptional changes are context-dependent[37] and rely on the relative quantities of interacting proteins like IκBα.[38] We observed that while quiescent ECs induced moderate activation of

inflammatory pathways within target cancer cells and inhibited the proliferation and invasion of cancer cells, dysfunctional ECs induced more profound pro-inflammatory signaling during all time points examined. DECs stimulated cancer cell apoptosis, but the surviving cancer cells were very aggressive. Quiescent ECs may not be strictly anti-inflammatory, but rather might induce controlled inflammation, with balanced action of activating (e.g. NF-κB P65) and inhibiting (IκBα) components, to direct wound healing and cancer inhibition. Thus, just as in vascular disease and repair, ECs are capable of inhibiting tumor aggressiveness, but this inhibitory phenotype can be changed to a tumor stimulatory

phenotype. Future work should delineate more fully the differential NF-κB and STAT3 signaling dynamics induced within cancer cells by ECs of a range of phenotypes.

We have used matrix-embedded EC (MEEC) constructs to investigate paracrine regulatory processes in a wide range of injury[3, 4, 39] and tumor models.[6] A relatively small number (~1 million) of implanted matrix-embedded ECs modulate local tissue physiology without extravasation/invasion of the implanted cells into the host or immune rejection of the implants – testimony to the paracrine potency of ECs[23]. In prior work, quiescent MEEC implants guided repair, limited morphological and immunohistochemical markers of malignancy and of metastatic potential, and restrained cancer progression.[6] Here, dysfunctional EC constructs stimulated pro-inflammatory signaling within adjacent tumors and significantly increased spontaneous metastasis. These findings are in line with the notion of a cancer-inhibitory physiologic microenvironment[40] that is eventually co-opted by tumors and are a direct extension of the context-dependent regulatory effects in vascular disease, wherein quiescent ECs suppress and dysfunctional endothelial cells stimulate diverse disease processes.

The use of intact cells rather than isolated molecules offers the opportunity to affect cancer biology broadly, but also poses a challenge in defining specific mechanism(s). It is appealing to search for a single molecule or pathway to define a cellular effect. Indeed, we previously showed that controlled disruption of the endothelial phenotype – via silencing of the gene encoding perlecan, a heparan sulfate proteoglycan critical for endothelial inhibition of thrombosis after vascular injury[17] – eliminated EC ability to inhibit cancer invasion and metastasis. EC secretion of IL-6, which is known to stimulate metastasis[20, 41], increases when the quiescent phenotype is disrupted and with perlecan silencing.[6] Yet, the IL-6 upregulation can also be seen with general stress and chemotherapy[42] and neutralization of IL-6 activity in DEC medium had no effect on induction of apoptosis in cancer cells. Paracrine regulatory effects are determined by the coordinated activity of the cell secretome, and many canonical signaling pathways are densely interconnected.[32] In contrast to dosing with isolated biologic factors, intact cells release a spectrum of regulatory molecules in a dynamic manner and in temporally and physiologically relevant proportions. The EC and DEC effects on cancer and vascular biology likely represent synergistic effects.[43]

Thus, these studies may implicate dysfunctional stromal ECs as active contributors to the tumor microenvironment and explain how anti-angiogenic therapies that damage the vasculature may shrink tumors and add months to patient survival[44] but under some circumstances stimulate cancer invasion and metastasis.[45, 46] The perceived role of ECs in cancer is expanding from the structural lining of tumor-perfusing blood vessels to a stromal paracrine regulatory element.[24, 47–50] Future work will help define how the tumor microenvironment can make endogenous tumor-associated endothelium dysfunctional and what specific endothelial-derived products may dominate particular cancer-regulatory phenomena. Such studies may illustrate deeper similarities between the tumor endothelial phenotype and the dysfunctional endothelial phenotype observed in diverse diseases including atherosclerosis, hypertension, and diabetes. They may also implicate previously-unforeseen consequences stemming from therapies that target the tumor vasculature. Lessons learned may motivate the development of novel pharmacologic or cell-based interventions – or the redirecting of therapies that regulate endothelial health – to slow or reverse tumor progression.

Supplementary Material

Refer to Web version on PubMed Central for supplementary material.

Acknowledgments

The authors thank Professors Angelo Cardoso, David Housman, David Scadden, and Sangeeta Bhatia for discussion and guidance.

Sources of funding: E.R.E. is supported by NIH R01 GM49039, V.C.C. by NIH-NIDDK (1K08DK080946) and a National Kidney Foundation Young Investigator Training Grant Award, and J.W.F. by NIH MSTP funding.

References

1. Michiels C. Endothelial cell functions. J Cell Physiol. 2003; 196:430–43. [PubMed: 12891700]
2. Rogers C, Parikh S, Seifert P, Edelman ER. Endogenous cell seeding. Remnant endothelium after stenting enhances vascular repair. Circulation. 1996; 94:2909–14. [PubMed: 8941120]
3. Nathan A, Nugent MA, Edelman ER. Tissue engineered perivascular endothelial cell implants regulate vascular injury. Proc Natl Acad Sci U S A. 1995; 92:8130–4. [PubMed: 7667257]
4. Zani BG, Kojima K, Vacanti CA, Edelman ER. Tissue-engineered endothelial and epithelial implants differentially and synergistically regulate airway repair. Proc Natl Acad Sci U S A. 2008; 105:7046–51. [PubMed: 18458330]
5. Carmeliet P, Jain RK. Principles and mechanisms of vessel normalization for cancer and other angiogenic diseases. Nat Rev Drug Discov. 2011; 10:417–27. [PubMed: 21629292]
6. Franses JW, Baker AB, Chitalia VC, Edelman ER. Stromal endothelial cells directly influence cancer progression. Sci Transl Med. 2011; 3:66ra5.
7. Libby P. Inflammation in atherosclerosis. Nature. 2002; 420:868–74. [PubMed: 12490960]
8. Ingber DE. Mechanical signaling and the cellular response to extracellular matrix in angiogenesis and cardiovascular physiology. Circ Res. 2002; 91:877–87. [PubMed: 12433832]
9. Carmeliet P, Dor Y, Herbert JM, Fukumura D, Brusselmans K, Dewerchin M, Neeman M, Bono F, Abramovitch R, Maxwell P, Koch CJ, Ratcliffe P, et al. Role of HIF-1alpha in hypoxia-mediated apoptosis, cell proliferation and tumour angiogenesis. Nature. 1998; 394:485–90. [PubMed: 9697772]
10. Bhowmick NA, Neilson EG, Moses HL. Stromal fibroblasts in cancer initiation and progression. Nature. 2004; 432:332–7. [PubMed: 15549095]
11. Zhang H, Park Y, Wu J, Chen X, Lee S, Yang J, Dellsperger KC, Zhang C. Role of TNF-alpha in vascular dysfunction. Clin Sci (Lond). 2009; 116:219–30. [PubMed: 19118493]
12. Bates DO. Vascular endothelial growth factors and vascular permeability. Cardiovasc Res. 2010; 87:262–71. [PubMed: 20400620]
13. van Beijnum JR, Dings RP, van der Linden E, Zwaans BM, Ramaekers FC, Mayo KH, Griffioen AW. Gene expression of tumor angiogenesis dissected: specific targeting of colon cancer angiogenic vasculature. Blood. 2006; 108:2339–48. [PubMed: 16794251]
14. Albini A, Benelli R. The chemoinvasion assay: a method to assess tumor and endothelial cell invasion and its modulation. Nat Protoc. 2007; 2:504–11. [PubMed: 17406614]
15. Meylan E, Dooley AL, Feldser DM, Shen L, Turk E, Ouyang C, Jacks T. Requirement for NF-kappaB signalling in a mouse model of lung adenocarcinoma. Nature. 2009; 462:104–7. [PubMed: 19847165]
16. O'Reilly MS, Holmgren L, Shing Y, Chen C, Rosenthal RA, Moses M, Lane WS, Cao Y, Sage EH, Folkman J. Angiostatin: a novel angiogenesis inhibitor that mediates the suppression of metastases by a Lewis lung carcinoma. Cell. 1994; 79:315–28. [PubMed: 7525077]
17. Nugent MA, Nugent HM, Iozzo RV, Sanchack K, Edelman ER. Perlecan is required to inhibit thrombosis after deep vascular injury and contributes to endothelial cell-mediated inhibition of intimal hyperplasia. Proc Natl Acad Sci U S A. 2000; 97:6722–7. [PubMed: 10841569]
18. Zeisberg EM, Tarnavski O, Zeisberg M, Dorfman AL, McMullen JR, Gustafsson E, Chandraker A, Yuan X, Pu WT, Roberts AB, Neilson EG, Sayegh MH, et al. Endothelial-to-mesenchymal transition contributes to cardiac fibrosis. Nat Med. 2007; 13:952–61. [PubMed: 17660828]
19. Potenta S, Zeisberg E, Kalluri R. The role of endothelial-to-mesenchymal transition in cancer progression. Br J Cancer. 2008; 99:1375–9. [PubMed: 18797460]

20. Sansone P, Storci G, Tavolari S, Guarnieri T, Giovannini C, Taffurelli M, Ceccarelli C, Santini D, Paterini P, Marcu KB, Chieco P, Bonafe M. IL-6 triggers malignant features in mammospheres from human ductal breast carcinoma and normal mammary gland. J Clin Invest. 2007; 117:3988–4002. [PubMed: 18060036]
21. Yu H, Pardoll D, Jove R. STATs in cancer inflammation and immunity: a leading role for STAT3. Nat Rev Cancer. 2009; 9:798–809. [PubMed: 19851315]
22. Pierce JW, Schoenleber R, Jesmok G, Best J, Moore SA, Collins T, Gerritsen ME. Novel inhibitors of cytokine-induced IkappaBalpha phosphorylation and endothelial cell adhesion molecule expression show anti-inflammatory effects in vivo. J Biol Chem. 1997; 272:21096–103. [PubMed: 9261113]
23. Methe H, Nugent HM, Groothuis A, Seifert P, Sayegh MH, Edelman ER. Matrix embedding alters the immune response against endothelial cells in vitro and in vivo. Circulation. 2005; 112:I89–95. [PubMed: 16159871]
24. Butler JM, Kobayashi H, Rafii S. Instructive role of the vascular niche in promoting tumour growth and tissue repair by angiocrine factors. Nat Rev Cancer. 2010; 10:138–46. [PubMed: 20094048]
25. Dodge AB, Lu X, D'Amore PA. Density-dependent endothelial cell production of an inhibitor of smooth muscle cell growth. J Cell Biochem. 1993; 53:21–31. [PubMed: 8227180]
26. Nugent MA, Karnovsky MJ, Edelman ER. Vascular cell-derived heparan sulfate shows coupled inhibition of basic fibroblast growth factor binding and mitogenesis in vascular smooth muscle cells. Circ Res. 1993; 73:1051–60. [PubMed: 8222077]
27. Ruoslahti E. Specialization of tumour vasculature. Nat Rev Cancer. 2002; 2:83–90. [PubMed: 12635171]
28. Castermans K, Griffioen AW. Tumor blood vessels, a difficult hurdle for infiltrating leukocytes. Biochim Biophys Acta. 2007; 1776:160–74. [PubMed: 17888580]
29. Houle F, Huot J. Dysregulation of the endothelial cellular response to oxidative stress in cancer. Mol Carcinog. 2006; 45:362–7. [PubMed: 16637066]
30. Ghosh K, Thodeti CK, Dudley AC, Mammoto A, Klagsbrun M, Ingber DE. Tumor-derived endothelial cells exhibit aberrant Rho-mediated mechanosensing and abnormal angiogenesis in vitro. Proc Natl Acad Sci U S A. 2008; 105:11305–10. [PubMed: 18685096]
31. Grivennikov SI, Greten FR, Karin M. Immunity, inflammation, and cancer. Cell. 2010; 140:883–99. [PubMed: 20303878]
32. Hanahan D, Weinberg RA. Hallmarks of cancer: the next generation. Cell. 2011; 144:646–74. [PubMed: 21376230]
33. Libby P, Ridker PM, Hansson GK. Inflammation in atherosclerosis: from pathophysiology to practice. J Am Coll Cardiol. 2009; 54:2129–38. [PubMed: 19942084]
34. Rocha VZ, Libby P. Obesity, inflammation, and atherosclerosis. Nat Rev Cardiol. 2009; 6:399–409. [PubMed: 19399028]
35. Erez N, Truitt M, Olson P, Arron ST, Hanahan D. Cancer-Associated Fibroblasts Are Activated in Incipient Neoplasia to Orchestrate Tumor-Promoting Inflammation in an NF-kappaB-Dependent Manner. Cancer Cell. 2010; 17:135–47. [PubMed: 20138012]
36. Pitroda SP, Zhou T, Sweis RF, Filippo M, Labay E, Beckett MA, Mauceri HJ, Liang H, Darga TE, Perakis S, Khan SA, Sutton HG, et al. Tumor endothelial inflammation predicts clinical outcome in diverse human cancers. PLoS One. 2012; 7:e46104. [PubMed: 23056240]
37. Ashall L, Horton CA, Nelson DE, Paszek P, Harper CV, Sillitoe K, Ryan S, Spiller DG, Unitt JF, Broomhead DS, Kell DB, Rand DA, et al. Pulsatile stimulation determines timing and specificity of NF-kappaB-dependent transcription. Science. 2009; 324:242–6. [PubMed: 19359585]
38. Ferreiro DU, Komives EA. Molecular mechanisms of system control of NF-kappaB signaling by IkappaBalpha. Biochemistry. 2010; 49:1560–7. [PubMed: 20055496]
39. Nugent HM, Groothuis A, Seifert P, Guerraro JL, Nedelman M, Mohanakumar T, Edelman ER. Perivascular endothelial implants inhibit intimal hyperplasia in a model of arteriovenous fistulae: a safety and efficacy study in the pig. J Vasc Res. 2002; 39:524–33. [PubMed: 12566978]
40. Bissell MJ, Hines WC. Why don't we get more cancer? A proposed role of the microenvironment in restraining cancer progression. Nat Med. 2011; 17:320–9. [PubMed: 21383745]

41. Gao SP, Mark KG, Leslie K, Pao W, Motoi N, Gerald WL, Travis WD, Bornmann W, Veach D, Clarkson B, Bromberg JF. Mutations in the EGFR kinase domain mediate STAT3 activation via IL-6 production in human lung adenocarcinomas. J Clin Invest. 2007; 117:3846–56. [PubMed: 18060032]

42. Gilbert LA, Hemann MT. DNA damage-mediated induction of a chemoresistant niche. Cell. 2010; 143:355–66. [PubMed: 21029859]

43. Ettenson DS, Koo EW, Januzzi JL, Edelman ER. Endothelial heparan sulfate is necessary but not sufficient for control of vascular smooth muscle cell growth. J Cell Physiol. 2000; 184:93–100. [PubMed: 10825238]

44. Jain RK. Lessons from multidisciplinary translational trials on anti-angiogenic therapy of cancer. Nat Rev Cancer. 2008; 8:309–16. [PubMed: 18337733]

45. Ebos JM, Lee CR, Cruz-Munoz W, Bjarnason GA, Christensen JG, Kerbel RS. Accelerated metastasis after short-term treatment with a potent inhibitor of tumor angiogenesis. Cancer Cell. 2009; 15:232–9. [PubMed: 19249681]

46. Paez-Ribes M, Allen E, Hudock J, Takeda T, Okuyama H, Vinals F, Inoue M, Bergers G, Hanahan D, Casanovas O. Antiangiogenic therapy elicits malignant progression of tumors to increased local invasion and distant metastasis. Cancer Cell. 2009; 15:220–31. [PubMed: 19249680]

47. Folkman J. Tumor angiogenesis: therapeutic implications. N Engl J Med. 1971; 285:1182–6. [PubMed: 4938153]

48. Rak J, Filmus J, Kerbel RS. Reciprocal paracrine interactions between tumour cells and endothelial cells: the ‘angiogenesis progression’ hypothesis. Eur J Cancer. 1996; 32A:2438–50. [PubMed: 9059332]

49. Bandyopadhyay S, Zhan R, Chaudhuri A, Watabe M, Pai SK, Hirota S, Hosobe S, Tsukada T, Miura K, Takano Y, Saito K, Pauza ME, et al. Interaction of KAI1 on tumor cells with DARC on vascular endothelium leads to metastasis suppression. Nat Med. 2006; 12:933–8. [PubMed: 16862154]

50. Calabrese C, Poppleton H, Kocak M, Hogg TL, Fuller C, Hamner B, Oh EY, Gaber MW, Finklestein D, Allen M, Frank A, Bayazitov IT, et al. A perivascular niche for brain tumor stem cells. Cancer Cell. 2007; 11:69–82. [PubMed: 17222791]

Novelty, impact

This work describes how dysfunctionally activated and inflamed endothelial cells can stimulate cancer aggression, just as similarly activated endothelial cells stimulate atherogenesis. This work adds to known roles of endothelial cells in cancer while showing how insights into non-malignant vascular biology may guide future work in the vascular biology of cancer.

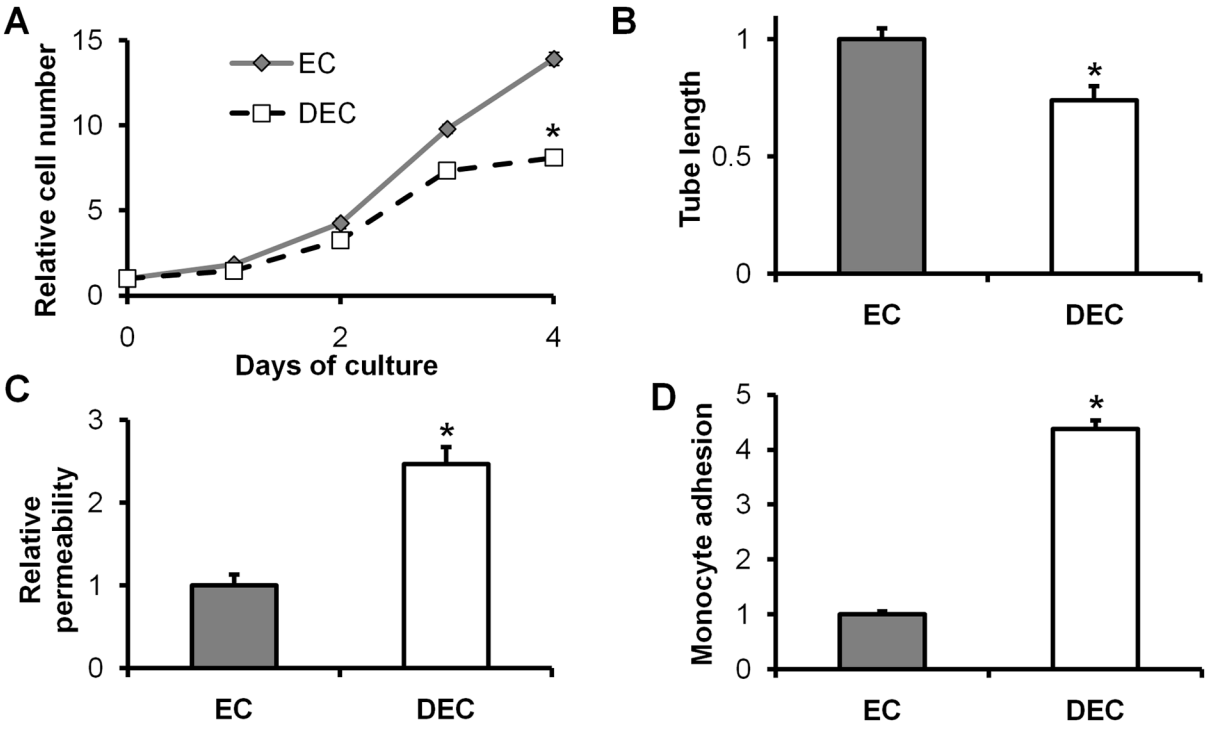

Figure 1. The in vitro "dysfunctional" EC (DEC) phenotype includes dysregulated proliferation, tube formation, high permeability, and avid monocyte binding

(A) Growth curve of endothelial cells cultured under intact ("EC") or dysfunctional ("DEC") *in vitro* conditions. (B) Tube length per field of ECs and DECs after 2 days of culture. (C) Permeability to the passage of FITC-dextran of confluent EC or DEC monolayers after 4 days of culture. (D) Adhesion of THP-1 monocytic leukemia cells to confluent EC or DEC monolayers after 4 days of culture. * $p<0.05$ versus EC by t test. n = 4 per condition.

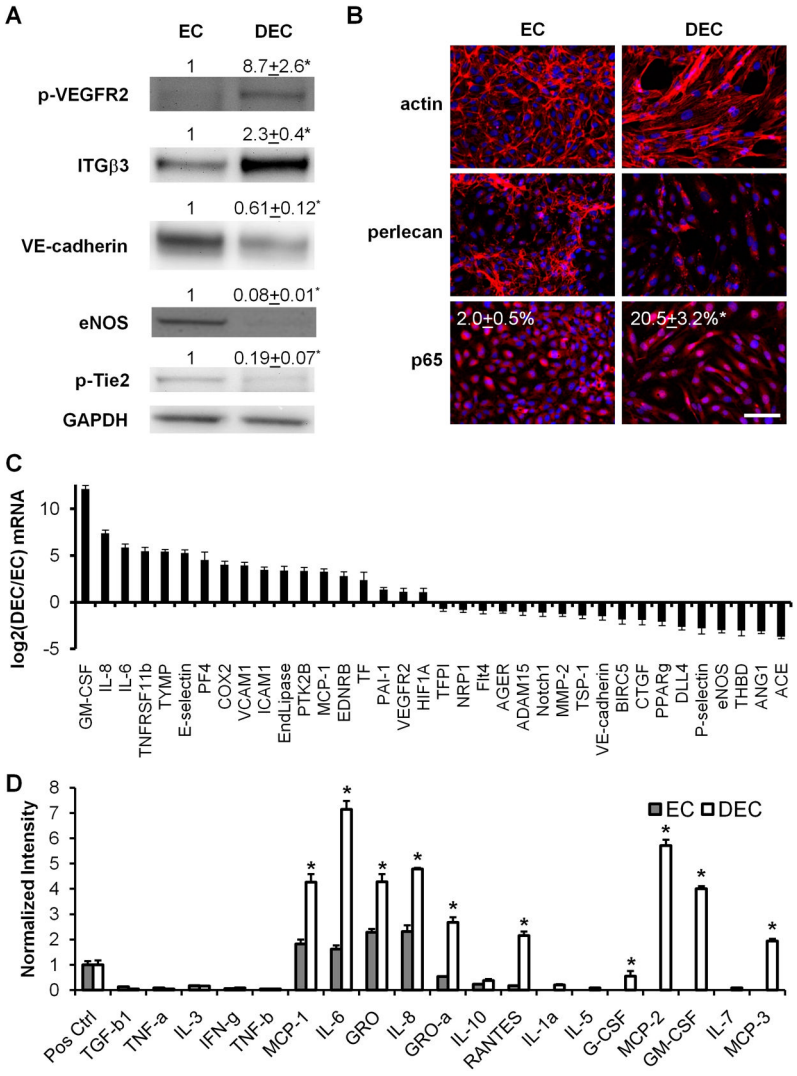

Figure 2. The DEC phenotype manifests in increased dysfunctional indices, reduced quiescent indices, altered and inflamed morphology, and highly pro-inflammatory and pro-thrombotic expression profiles

(A) Western blot of whole cell lysates of ECs and DECs, with quantification for DEC lysates relative to EC lysates. (B) Immunofluorescent staining for actin (fluorescent phalloidin), perlecan, and NF-κB p65 in ECs and DECs. Nuclei are labeled in blue (DAPI). (C) qRT-PCR array analysis of endothelial inflammatory, thrombotic, and quiescent differentiation genes. (D) Cytokine dot blot of EC and DEC secretions. * $p<0.05$ by t test. n = 3 per condition.

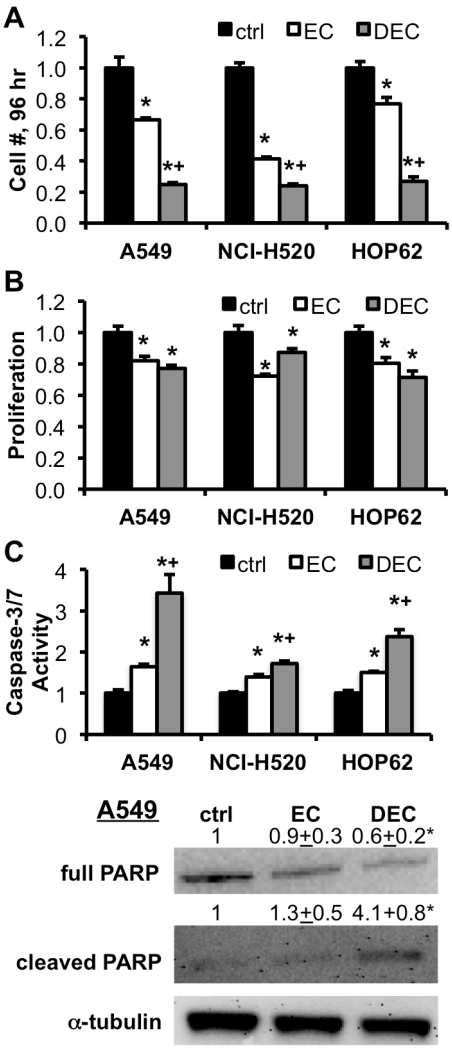

Figure 3. ECs inhibit cancer cell proliferation, but pro-inflammatory DECs induce cancer cell death

(A) MTT assay of the A549, NCI-H520, and HOP62 lung carcinoma cells after 4 days of culture in either unconditioned (control), EC-conditioned, or DEC-conditioned media. (B) BrdU incorporation of the same cells during hours 24–48 of culture in the same sets of conditioned media. (C) Caspase-3/7 activity in A549, NCI-H520, and HOP62 cells, and Western blot of full and cleaved PARP in A549 cells, after 4 hours of culture. * $p<0.05$ versus control, $^{+}$ $p<0.05$ versus EC by t test. n = 3 per condition.

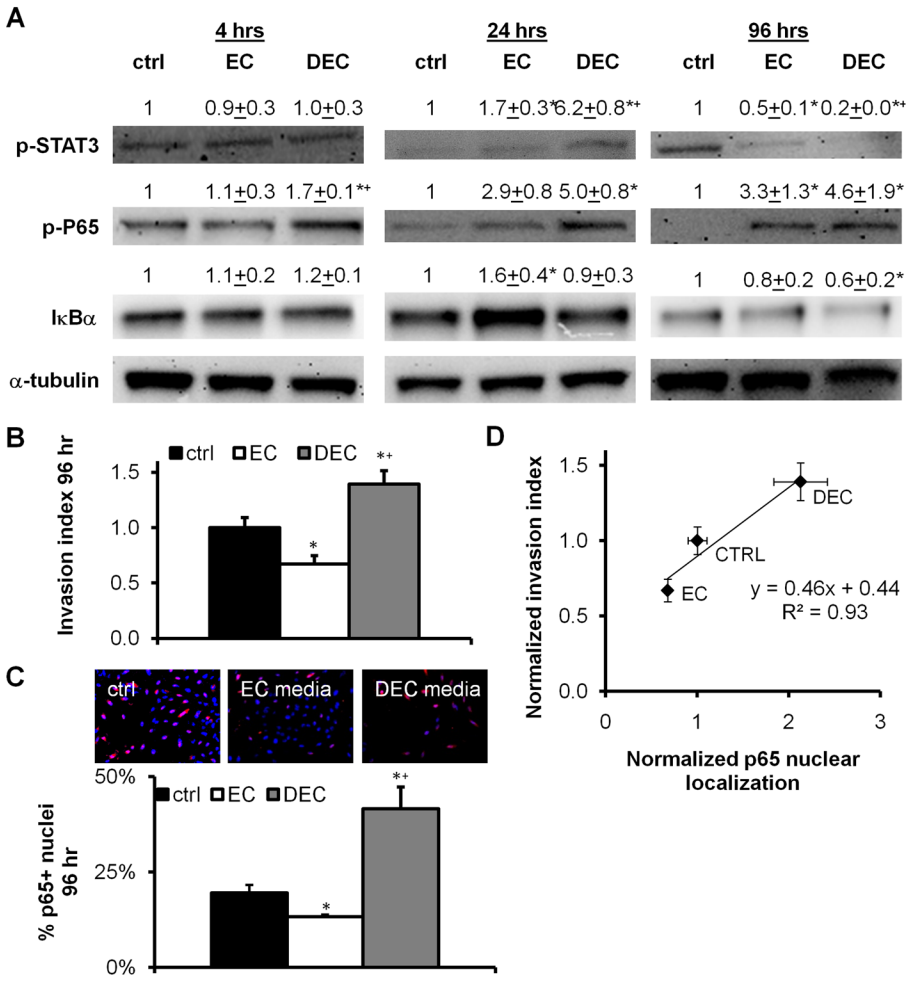

Figure 4. ECs control lung cancer inflammatory signaling and reduce invasiveness, whereas DECs robustly stimulate lung cancer inflammatory signaling and stimulate invasiveness

(A) Time course of STAT3 (p-STAT3) and NF-κB pathway activity (p-P65 and IκBα) induced by unconditioned (control), EC-conditioned, or DEC-conditioned media as assayed by Western blot of whole cell lysates of A549 cells. Quantification, relative to control, is shown above each representative band. (B) In vitro chemoinvasion index of A549 cells after 4 days of culture in the same sets of conditioned media. (C) Immunofluorescent nuclear localization of NF-κB p65 in A549 cells after 4 days of culture in the same sets of conditioned media. (D) Correlation between effects of EC or DEC secretions on A549 invasiveness and NF-κB p65 nuclear localization. * $p<0.05$ versus control, $^{+}$ $p<0.05$ versus EC by t test. n = 3 per condition.

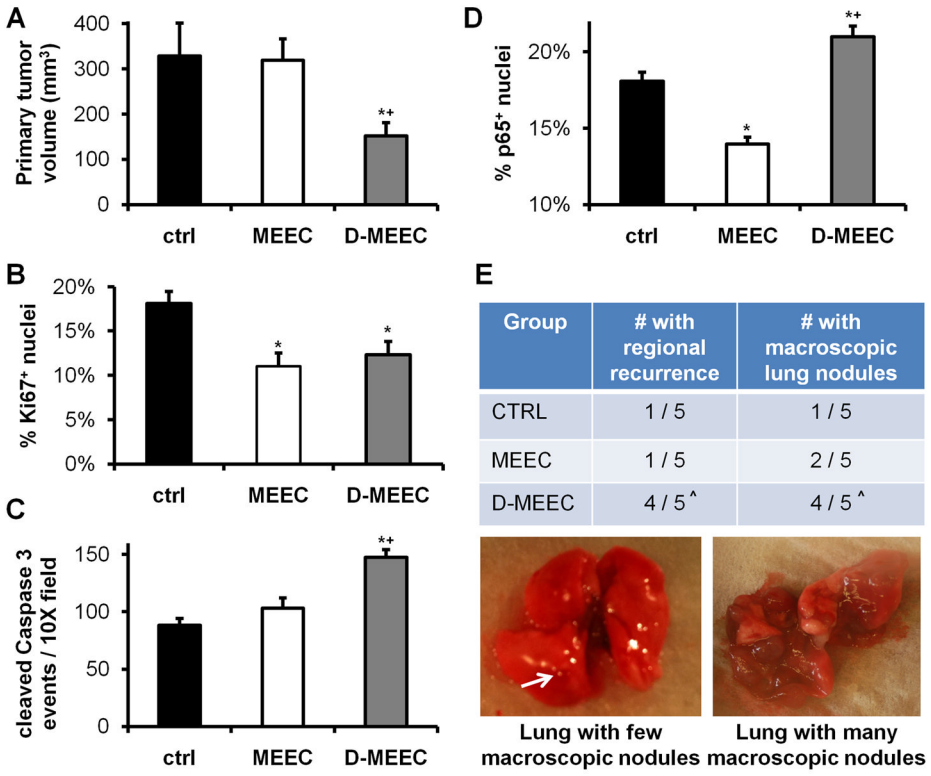

Figure 5. Adjacent D-MEECs cause increased spontaneous metastases and in parallel slow the net growth of primary tumors

(A) Tumor volumes estimated by caliper measurements of explanted Lewis lung carcinoma tumors. (B) Percent of Ki67-positive nuclei of thresholded immunofluorescent primary tumor cryosection images. (C) Numbers of host (murine) cleaved caspase 3 events per 10X field of immunofluorescent primary tumor cryosections. (D) Percent of NF-κB p65-positive nuclei of immunofluorescent primary tumor cryosections. (E) Table showing fractions of mice with macroscopic regional (posterior cervical) metastasis and with pan-lobar macroscopic lung metastases 2 weeks after primary tumor resection. * $p<0.05$ versus control by t test. $^{+}$ $p<0.05$ versus MEEC by t test. $^{\wedge}$ $p<0.05$ by proportion z-test. n = 6 per condition.

Table 1

Primer sequences for qRT-PCR gene expression analysis.

Gene	Forward Primer (5′-3′)	Reverse Primer (5′-3′)
GAPDH	ACAGTCAGCCGCATCTTCTT	TGGAAGATGGTGATGGGATT
Twist1	ATCAAACTGGCCTGCAAAAC	TGCATTTTACCATGGGTCCT
Snail	CTAGAGTCTGAGATGCCCCG	GTTCTGGGAGACACATCGGT
Slug	CTTTTTCTTGCCCTCACTGC	GCTTCGGAGTGAAGAAATGC
Sip1	ATTGGTTTTCCTCCCTTGCT	AAGCAGGAACCCTCTCATCA
IL-6	CACAAGCGCCTTCGGTCCAGTT	TCTGCCAGTGCCTCTTTGCTGC
THBD	ACTGTGACTCCGGCAAGGTGGA	AAAAGCGCCACCACCAGGCA
eNOS	TTGCTCGTGCCGTGGACACA	TGGCGCTTCCAGCTCCGTTT
E-selectin	AACCCCGAGCGAGGCTACATGA	ACACAGTGCCAAACACGGGCTC